Cell

Cell Surface- and Rho GTPase-Based Auxin Signaling Controls Cellular Interdigitation in *Arabidopsis*

Tongda Xu,[1] Mingzhang Wen,[1] Shingo Nagawa,[1] Ying Fu,[1] Jin-Gui Chen,[2] Ming-Jing Wu,[2] Catherine Perrot-Rechenmann,[3] Jiří Friml,[4] Alan M. Jones,[2,5] and Zhenbiao Yang[1,*]
[1]Center for Plant Cell Biology, Department of Botany and Plant Sciences, University of California, Riverside, CA 92521, USA
[2]Department of Biology, The University of North Carolina at Chapel Hill, Chapel Hill, North Carolina 27599, USA
[3]Institut des Sciences du Végétal, CNRS, UPR2355, 1 Avenue de la Terrasse, 91198 Gif sur Yvette Cedex, France
[4]Department of Plant Systems Biology, VIB, and Department of Molecular Genetics, Ghent University, Technologiepark 927, 9052 Gent, Belgium
[5]Department of Pharmacology, The University of North Carolina at Chapel Hill, Chapel Hill, North Carolina 27599, USA
*Correspondence: yang@ucr.edu
DOI 10.1016/j.cell.2010.09.003

SUMMARY

Auxin is a multifunctional hormone essential for plant development and pattern formation. A nuclear auxin-signaling system controlling auxin-induced gene expression is well established, but cytoplasmic auxin signaling, as in its coordination of cell polarization, is unexplored. We found a cytoplasmic auxin-signaling mechanism that modulates the interdigitated growth of *Arabidopsis* leaf epidermal pavement cells (PCs), which develop interdigitated lobes and indentations to form a puzzle-piece shape in a two-dimensional plane. PC interdigitation is compromised in leaves deficient in either auxin biosynthesis or its export mediated by PINFORMED 1 localized at the lobe tip. Auxin coordinately activates two Rho GTPases, ROP2 and ROP6, which promote the formation of complementary lobes and indentations, respectively. Activation of these ROPs by auxin occurs within 30 s and depends on AUXIN-BINDING PROTEIN 1. These findings reveal Rho GTPase-based auxin-signaling mechanisms, which modulate the spatial coordination of cell expansion across a field of cells.

INTRODUCTION

Auxin regulation of plant growth and development requires a nuclear signaling mechanism, which involves auxin stabilizing the interaction between the TIR1-family F box proteins and the IAA/AUX transcriptional repressors, leading to IAA/AUX degradation and changes in gene expression (Leyser, 2006; Parry and Estelle, 2006; Dharmasiri et al., 2005a; Kepinski and Leyser, 2005; Mockaitis and Estelle, 2008; Tan et al., 2007). However, this pathway cannot account for auxin-induced rapid cellular responses occurring within minutes, such as cell expansion, cytosolic Ca^{2+} increase, and proton secretion (Badescu and Napier, 2006; Senn and Goldsmith, 1988; Shishova and Lindberg, 2004; Vanneste and Friml, 2009). AUXIN BINDING PROTEIN1 (ABP1) has been proposed to be an auxin receptor that rapidly activates cell expansion (Badescu and Napier, 2006; Chen et al., 2001a, 2001b; Jones, 1994). ABP1 knockout causes lethality of early embryos due to their failure to polarize (Chen et al., 2001b). Auxin is also implicated in the regulation of cell polarization including polar distribution of the auxin efflux facilitator PIN (PINFORMED) proteins to the plasma membrane (PM) and determination of root hair initiation sites in the root epidermal cells (Dhonukshe et al., 2008; Fischer et al., 2006; Paciorek et al., 2005). However, signaling events downstream of ABP1 and those underlying the control of cell polarization by auxin are unknown.

Coordinated spatial control of cell expansion or asymmetry across an entire field of cells in a tissue is important for pattern formation and morphogenesis. In animals, this type of spatial coordination is required for cellular intercalation that drives convergent extensions during early embryogenesis (Green and Davidson, 2007; Heasman, 2006). In plants, PIN proteins are located to one cell end in a specific tissue to generate directional flow of auxin (Petrasek et al., 2006; Wisniewska et al., 2006). In addition, spatial coordination among epidermal cells is important for patterning of the epidermal tissues such as the positioning of root hairs and the jigsaw-puzzle appearance of pavement cells (PCs) in the leaf (Fischer et al., 2006; Fu et al., 2005, 2002). The molecular mechanisms underlying the spatial coordination in these plant systems are poorly understood.

We used *Arabidopsis* leaf epidermal PCs as a model system to investigate the mechanisms for the cell-cell coordination of interdigitated cell expansion (Fu et al., 2005, 2002; Settleman, 2005; Yang, 2008). The jigsaw-puzzle appearance results from intercalary growth that produces interdigitated lobes and indentations (Figure 1A). This cellular interdigitation resembles embryonic cell intercalation required for convergent extension in animal cells. Interestingly, these two distinct processes share common mechanisms, including Rho GTPase signaling and its effect on

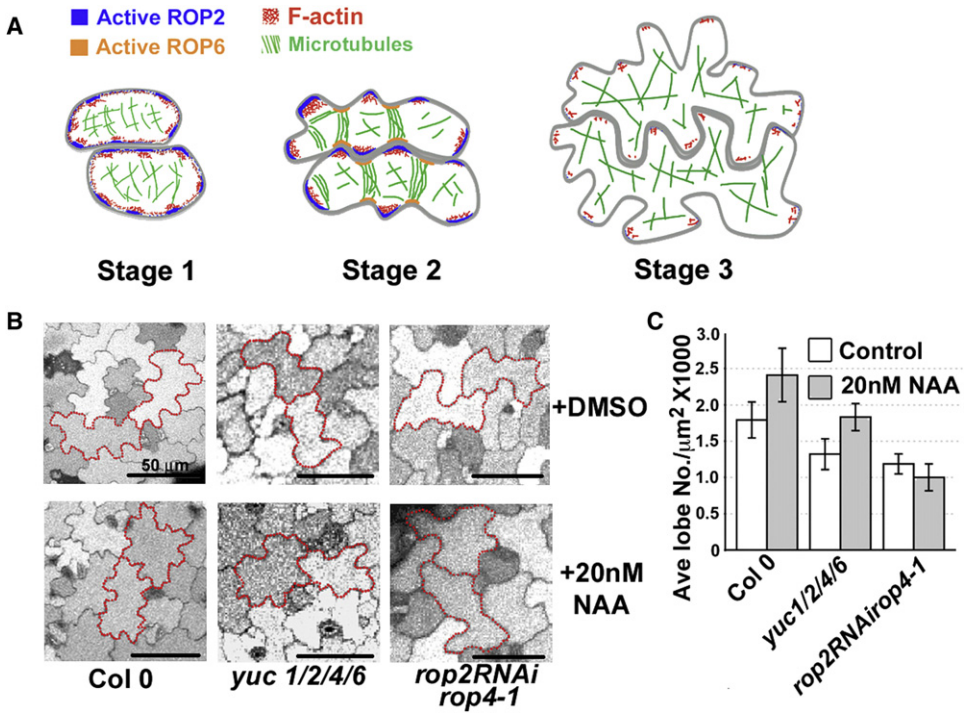

Figure 1. Auxin Activation of PC Interdigitation Requires ROP2/4

(A) A schematic showing three stages of PC morphogenesis as described (Fu et al., 2005).

(B) Auxin increased interdigitation of WT PCs and suppresses the PC interdigitation defect in the *yuc1 yuc2 yuc4 yuc6* (*yuc 1/2/4/6*) quadruple mutant but not in the *ROP2RNAi rop4-1*. Seedlings were cultured in liquid MS with or without 20 nM NAA, and cotyledon PCs were imaged 4 days after stratification.

(C) Quantitative analysis of PC interdigitation. The degree of interdigitation in PCs shown in (B) was quantified by determining the density of lobes for each PC (Figure S1A). Data are mean lobe number per $\mu m^2 \pm$ SD ($n > 400$ cells from three individual plants). The *yuc* mutant had a significantly lower density of lobes than Col-0 wild-type, and NAA significantly increased the mean density of lobes in Col-0 WT and the *yuc* mutant (t test, $p < 0.001$) but not in the *ROP2RNAi rop4-1* line (t test, $p > 0.1$). Nonbiased double blind analysis confirms all of the phenotypic differences between mutants and treatments (Figure S1B).

Also see Figure S1.

the cytoskeleton (Fu et al., 2005; Settleman, 2005; Yang, 2008). ROP2 and ROP4, two functionally-overlapping members of the Rho GTPase family in *Arabidopsis*, promote lobe development (Fu et al., 2005, 2002). ROP2, locally active at the lobe-forming site, promotes the formation of cortical diffuse F-actin and lobe outgrowth via its effector RIC4 (Fu et al., 2005). In the lobe tips, ROP2 suppresses well-ordered cortical microtubule (MT) arrays by inactivating another effector, RIC1 (Fu et al., 2005, 2002), thus relieving MT-mediated outgrowth inhibition. In the opposing indenting zone, ROP6 activates RIC1 to promote well-ordered MTs and to suppress ROP2 activation (Fu et al., 2005, 2009). What activates the ROP2 and ROP6 pathways and how these two pathways coordinate across cells to produce the cellular interdigitation remains unknown.

In this report, we demonstrate that auxin promotes interdigitated PC expansion by coordinately activating the antagonistic ROP2 and ROP6 pathways in an ABP1-dependent manner and that ROP2 is required for the targeting of PIN1 to the lobing regions of the PM, which is crucial for the interdigitated PC expansion. These findings establish a molecular framework underpinning cellular interdigitation as well as an auxin-signaling mechanism that is downstream of ABP1 and required for cytoplasmic events including cytoskeletal organization, PIN protein targeting, and spatially coordinated cell expansion.

RESULTS

Auxin Promotes and Is Required for PC Interdigitation

Given the widespread role of auxin in plant pattern formation, we evaluated its involvement in the interdigitated growth of PCs in *Arabidopsis*. We first examined the effect of exogenous auxin on the degree of PC interdigitation, which was measured by the number of lobes per cell area in a two-dimensional plane of the leaf surface (Figure S1A available online). Treatments of wild-type (WT) seedlings with the synthetic auxin naphthalene-1-acetic acid (NAA) significantly increased PC interdigitation in a dose-dependent manner with an effective NAA concentration as low as 5 nM and optimal concentration around 20 nM (Figures 1B and 1C and Figure S1C).The requirement of endogenous auxin for PC interdigitation was investigated using mutants defective in *YUCCA* gene family-dependent auxin biosynthesis (Cheng et al., 2006; Zhao et al., 2001). The cotyledon PCs of the *yuc1 yuc2 yuc4 yuc6* quadruple mutant, which accumulates a lower amount of auxin than the wild-type (Cheng et al., 2006),

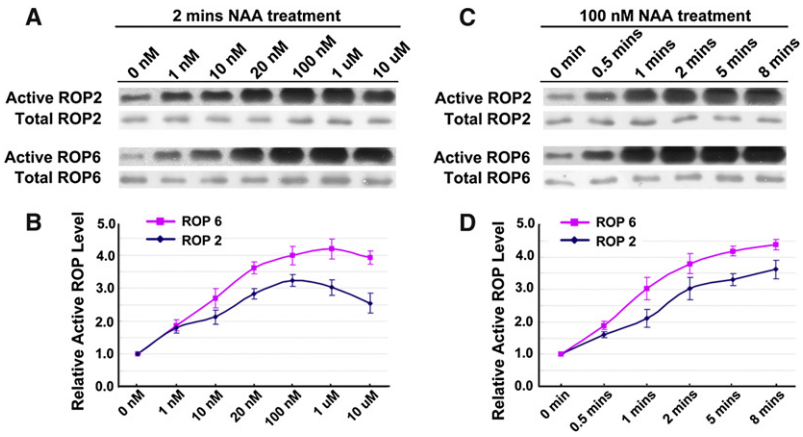

Figure 2. Auxin Rapidly Activates ROP2 and ROP6 in a Dosage-Dependent Manner

(A and C) Auxin dosage responses of ROP2 and ROP6 activation. Protoplasts from leaves of transgenic GFP-ROP2 or -ROP6 seedlings were treated with the indicated concentrations of NAA for 2 min (A), or treated with 100 nM NAA for the indicated times (C). GTP-bound active GFP-ROP2 or -ROP6 and total GFP-ROP2 or -ROP6 (GDP and GTP forms) were analyzed as described in text. Results from one out of five independent experiments with similar results are shown. ROP2 and ROP6 experiments were conducted in parallel under identical conditions.

(B and D) Quantitative analysis of data from (A) and (C). The relative ROP2 or ROP6 activity level was determined as the amount of GTP-bound ROP2 or ROP6 divided by the amount of total GFP-ROP2 or ROP6. The relative ROP activity in different treatments was standardized to that from mock-treated control, which was arbitrarily defined as "1." Data are mean activity levels from five independent experiments ± SD. We tested the significance of difference in ROP activity level between ROP2 and ROP6 at various auxin levels using F-test. All the p values are less than 0.001 except at 0 and 1 nM of auxin. We also compared mean values of ROP activity level using Tukey pairwise mean comparisons and found that ROP2 activity significantly increased at lower auxin levels, stabilized at median auxin levels, and significantly decreased at high auxin levels. In contrast, ROP6 activity significantly increased at low and median levels and stabilized at high auxin levels.

Also see Figure S2.

exhibited reduced interdigitation (Figures 1B and 1C). This *yuc1 yuc2 yuc4 yuc6* PC phenotype resembled that of the *ROP2RNAi rop4-1* line (Figures 1B and 1C), in which *ROP2* and *ROP4* expression is reduced (Fu et al., 2005). Interestingly, NAA treatment rescued the interdigitation defect of the *yuc* quadruple mutant but not that of the *ROP2RNAi rop4-1* line (Figures 1B and 1C; Figures S1C and S1D). These results suggest that auxin is a signal that induces lobe formation possibly by activating ROP2 and ROP4.

Auxin Activates the ROP2-RIC4 Pathway at the PM

To test whether auxin activates ROP2, we first determined the effect of auxin on ROP2 activity using an effector binding-based assay (Baxter-Burrell et al., 2002) to measure active GTP-bound GFP-ROP2 in protoplasts isolated from *Arabidopsis* leaves stably expressing GFP-ROP2. We found that ROP2 activity doubled by addition of as low as 1 nM NAA and reached saturation at 20–100 nM NAA (Figures 2A and 2B), which is consistent with the concentrations of NAA for the induction of PC interdigitation (Figures S1C and S1F). Time course analysis showed that ROP2 activity doubled within 30 s after NAA treatment (Figure 2C and 2D). This is one of the most rapid auxin responses known to date, which suggests that auxin perception directly leads to ROP2 activation at the PM.

Localization of GFP-RIC4 to the PM is a display of in vivo activation of ROP2, because RIC4 specifically binds the active form of PM-delimited ROPs (Fu et al., 2005; Hwang et al., 2005). In wild-type PCs, GFP-RIC4 was preferentially localized to the PM domains associated with initiating or growing lobes where ROP2 is activated. In the *yuc* quadruple mutant, GFP-RIC4 localization to these PM domains was reduced, with a corresponding increase of its level in the cytoplasm (Figures S2A and S2B). Treatment with 20 nM auxin increased PM-associated GFP-RIC4 in this mutant (Figures S2A and S2B), but not in the *rop2-1 rop4-1* double mutant (data not shown). Fine cortical F-actin, a RIC4 signaling target, was also markedly reduced in the *yuc* quadruple-mutant PCs as in the *ROP2RNAi rop4-1* PCs (Fu et al., 2005) (Figure S2C). Taken together, our results indicate that auxin is required for localized ROP2 activation in the lobing region of PCs.

ABP1 Is Required for Auxin Promotion of PC Interdigitation

There are two well-characterized receptor families in *Arabidopsis*, ABP1 and TIR1 proteins. The TIR1-family of F box proteins directly controls auxin-induced gene expression (Leyser, 2006; Mockaitis and Estelle, 2008) and is unlikely to mediate ROP2 activation and other responses that are rapidly induced by auxin within 30 s (Badescu and Napier, 2006), since the most rapid auxin-induced changes in mRNA expression occur within 2-5 min after auxin treatments (Abel and Theologis, 1996). ABP1 is partially localized to the outer surface of the PM by associating with a GPI-anchored PM protein (Badescu and Napier, 2006; Jones, 1994; Shimomura, 2006; Steffens et al., 2001). Because null alleles of *abp1* are embryo lethal (Chen et al., 2001b), we isolated a weak allele, *abp1-5,* containing a point mutation (His94- > Tyr) in the auxin-binding pocket (Woo et al., 2002) (Figure 3A). PCs of *abp1-5* cotyledons showed a defect similar to that observed in the *yuc* quadruple mutant (Figure 3B and 3C**;** Figure 1B and 1C). This defect was rescued to WT by transgenic expression of *ABP1* (Figure S3A and S3B), confirming that the *abp1-5* defect was due to the *abp1-5* mutation. The role of ABP1 in PC interdigitation was further confirmed by inducible expression of an *ABP1* antisense RNA and a RNA encoding single-chain fragment variable 12 derived from anti-ABP1 mAb12 antibody (Braun et al., 2008) (Figures 3D and 3E and Figures S3C and S3D). Unlike PCs in the *yuc* quadruple mutant, exogenous auxin did not induce lobe formation in PCs containing the *abp1-5* mutation or expressing *ABP1* antisense RNA (Figures 3B–3E and Figure S1E). Thus,

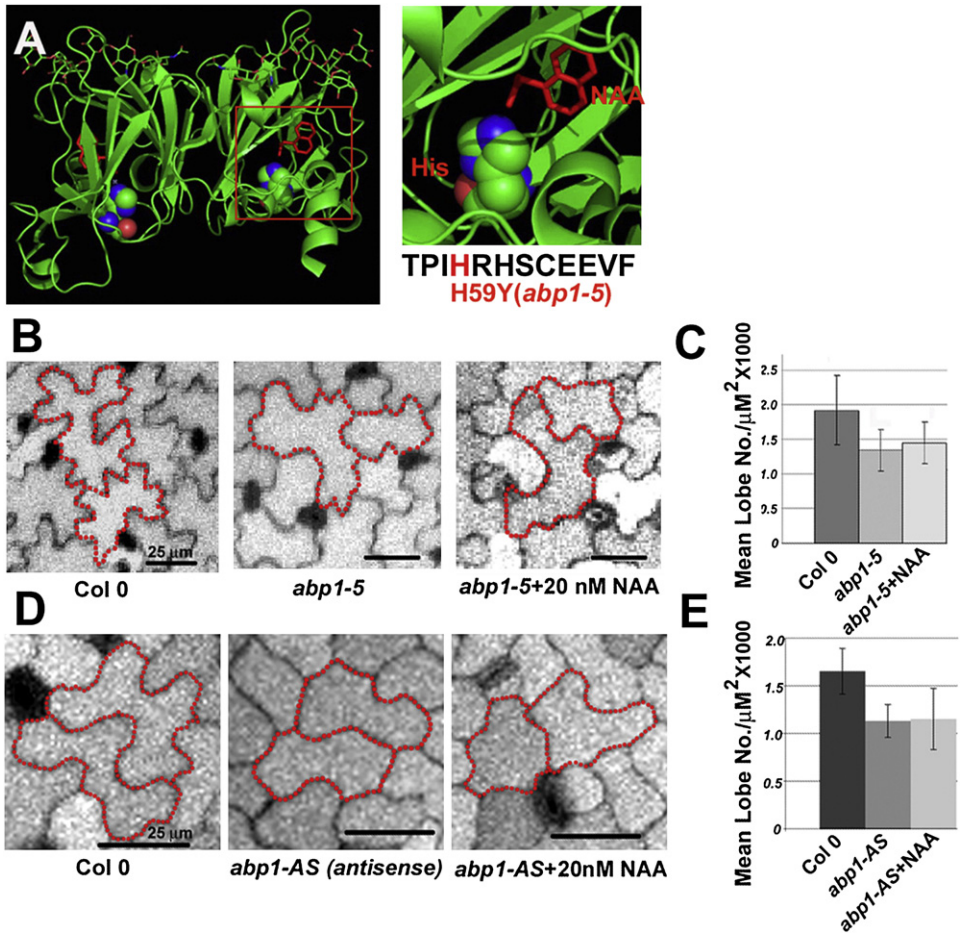

Figure 3. ABP1 Is Required for Auxin Perception that Promotes PC Interdigitation

(A) The *abp1-5* mutation (His59- > Tyr) occurs within the auxin binding pocket (Woo et al., 2002). (Left) The crystal structure of maize ABP1 with bound NAA (PDB 1lrh). Maize ABP1 is a glycosylated homodimer that binds two NAA molecules (shown in red). Maize and *Arabidopsis* share 68% identity overall and 100% conservation in the binding pocket. (Right) The auxin-binding pocket is highlighted to show how H59 (sphere format) interacts with the carboxic acid group of NAA shown in red and with a zinc ion not shown (for clarity).

(B) Defect in PC interdigitation in the *abp1-5* mutant was not rescued by auxin. Seedlings were cultured in liquid MS with or without 20 nM NAA, and cotyledon PCs were imaged 4 days after stratification.

(C) PC interdigitation shown in (B) was quantitated as in Figure 1C ($n > 400$ cells from three individual plants). WT had significantly higher lobe intensity than *abp1-5* (t test, $p < 0.001$). No significant difference was found between treatment with or without NAA (t test, $p > 0.1$).

(D) The defect in PC interdigitation in an inducible *ABP1* antisense line was not rescued by auxin. An *ABP1* antisense construct was expressed upon ethanol treatment (Braun et al., 2008). Seedlings were cultured in liquid MS containing 0.5% ethanol with or without NAA, and cotyledon PCs were imaged 4 days after stratification.Without ethanol treatment, the PCs in this line were similar to WT PCs (Figure S3C). Upon ethanol induction, *ABP1* antisense PCs were similar to the *abp1-5* cells and were not altered by NAA.

(E) PC interdigitation in the antisense line shown in (C) was quantitated as in Figure 1C ($n > 400$ cells from three individual plants). WT had a significantly higher lobe density than the *ABP1* antisense line in the absence of NAA (t test, $p < 0.001$), which did not show significant difference with NAA treatment (t test, $p > 0.1$). A double-blind analysis was performed and the results confirmed all of the phenotypic differences between mutants and treatments described in this figure (see Figure S3E).

we hypothesize that ABP1 perceives the auxin signal required for PC interdigitation.

ABP1 Is Required for Auxin Activation of the ROP2-RIC4 Pathway

We next tested whether ABP1 is required for the auxin activation of the ROP2 pathway. The *abp1-5* mutation greatly reduced GFP-RIC4 localization to the lobe tip and PM (Figures S4A and S4B), as well as localized accumulation of diffuse cortical F-actin (Figure S4C). Thus, ROP2 signaling is greatly compromised by *abp1-5*. Furthermore, the defect in RIC4 localization in the *abp1-5* mutant could not be rescued by auxin (Figure S4A). Finally, both the analysis of GFP-RIC4 localization and measurement of GTP-bound ROP2 showed that the rapid auxin activation of ROP2 in protoplasts was abolished by the *abp1-5* mutation and *ABP1* antisense expression (Figures 4A and 4B and Figures S4D–S4F). Hence, ABP1 acts upstream of ROP2 in the perception of auxin.

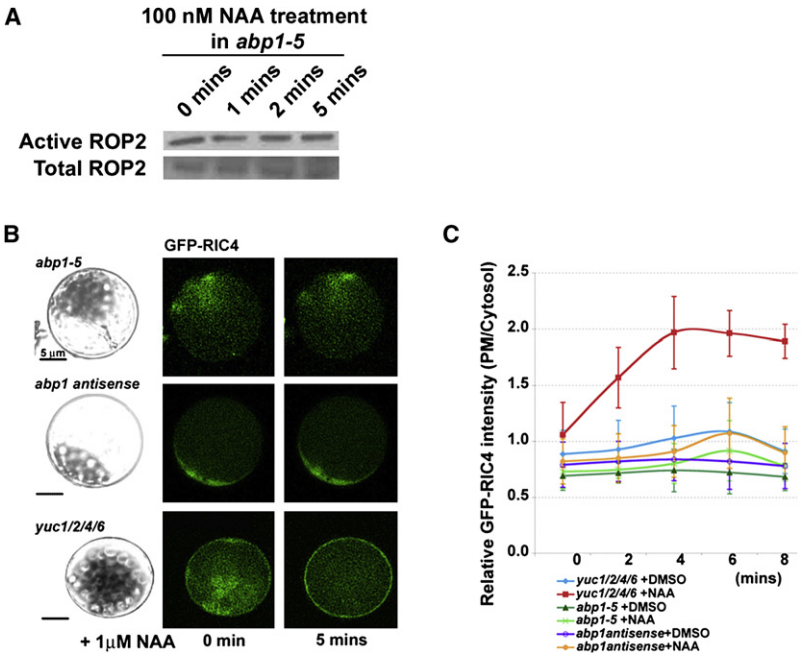

Figure 4. Auxin Can Activate ROP2-RIC4 Pathway through ABP1

(A) Measurement of GTP-bound GFP-ROP2 in protoplasts isolated from a *abp1-5* line stably expressing *35S::GFP-ROP2* by coimmunoprecipitation assay described in Figure 2. The seedlings expressing GFP and homozygous for *abp1-5* were pooled and used for protoplast isolation. Auxin did not activate ROP2 in *abp1-5* mutants compared to in wild-type where auxin activates ROP2 within 30 s (Figure 2C).

(B and C): Loss of auxin activation of ROP2 in the *abp1-5* mutant and the induced *ABP1* antisense line. GFP-RIC4 distribution to the PM in isolated protoplasts was used to report ROP2 activation by auxin. (**B**) Representative images of GFP-RIC4 distribution in protoplasts isolated from different lines before and 5 min after auxin application. The bright field images (left) show intact protoplasts corresponding to the GFP-RIC4 fluorescent images at time 0. See Figures S4D-S4F for representative images from the complete time course analysis. (**C**) Quantitative analysis of GFP-RIC4 distribution to the PM (as indicated by relative GFP intensity in the PM standardized with the cytosolic GFP intensity). Data are mean values from 10 protoplasts analyzed ± SD.

Also see Figure S4.

ROP2-Dependent Lobe-Localized PIN1 Is Required for Interdigitation

The presence of ABP1 at the cell surface (Diekmann et al., 1995; Jones and Herman, 1993; Leblanc et al., 1999) and ROP2 localization to the lobe PM imply that the perception of extracellular auxin leads to localized ROP2 activation. Thus, a mechanism for local accumulation of extracellular auxin is expected. In support of this notion, we found PIN1 preferentially localized to the PM of PC lobe tips (Figure 5A). PCs of a *PIN1* loss-of-function mutant, *pin1-1,* showed a defect in interdigitation, and were long and narrow (Figure 5B and Figures S5A and S5B), resembling the *ROP2RNAi rop4-1* line (Fu et al., 2005). Another allele, *pin1-5*, showed a similar phenotype (Figures S5E and S5F). GFP-RIC4 localization to the PM was compromised in the *pin1-1* mutant with GFP-RIC4 diffusely distributed in the cytosol (Figures 5D and 5E). Application of NAA failed to rescue the lobing defect in the *pin1-1* mutant (Figures 5B and 5C and Figures S5A and S5B), supporting a critical role for PIN1-mediated localized auxin export in lobe formation and localized ROP2 activation. This also implies a role for PIN1 in a positive feedback, i.e., PIN1 localization to the lobe tip may require ROP2 activation. Consistent with this implication, PIN1 localization to the PM was compromised in the *ROP2RNAi rop4-1* line, the *abp1-5* mutant, and the *ABP1* antisense line, which all showed greatly enhanced PIN1 internalization and reduced localization to the lobe PM (Figure 5A, right panel and Figures S5G and S5H). Transient expression of a dominant negative ROP2 mutant protein also increased PIN1-GFP internalization, suggesting that PIN1 localization to the PM is directly affected by ROP2 signaling, not indirectly through ROP2/4-mediated cell shape changes (Figures S5C and S5D). Taken together, these results support the hypothesis that a PIN1-dependent positive feedback loop is required for localized ROP2 signaling and lobe outgrowth. This also implies a role for localized extracellular auxin in the regulation of interdigitation.

Auxin Also Activates the ROP6-RIC1 Pathway in an ABP1-Dependent Manner

PIN1-exported auxin in the lobing side is expected to diffuse across the cell wall to the complementary side of the neighboring cell, where the ROP6-RIC1 pathway operates (Fu et al., 2009). We speculated that PIN1-exported auxin could serve as a cross-cell signal to activate the ROP6-RIC1 pathway, hence providing a mechanism for the cell-cell coordination of lobe outgrowth with indentation formation. Interestingly, the quadruple *yuc* and single *abp1-5* mutants exhibited an additional cell shape phenotype observed in *rop6-1* and *ric1-1* (Fu et al., 2005, 2009), specifically, wider neck regions (Figures 6A and 6B). The wide neck phenotype suggests that auxin and ABP1 may also activate the ROP6-RIC1 pathway, which promotes indenting. Thus we sought to test whether ABP1 perception of auxin activates the ROP6-RIC1 pathway.

ROP6 is required for RIC1 decoration of cortical MTs like beads on a string and for its function in promoting the ordering of cortical MTs (Fu et al., 2009). If auxin is required for ROP6 activation, one would expect that RIC1's association with cortical MTs is disrupted in the *abp1-5* and the *yuc* quadruple mutant, as in the *rop6-1* null mutant (Fu et al., 2009). Indeed, RIC1 association with cortical MTs was greatly abolished in both *yuc* quadruple and *abp1-5* single mutant PCs (Figure 6C and Figure S6A). Consistent with the defect of RIC1 distribution, the arrangement of cortical MTs in these mutants became mostly random, similar to that seen in *rop6-1* and *ric1-1* mutants (Figure S6B). This indicates that auxin and ABP1 are required for the activation of the ROP6-RIC1 pathway.

We next tested whether auxin promoted RIC1 association with cortical MTs. We previously showed that ROP2 inhibits RIC1 function by sequestering RIC1 from cortical MTs in PCs. To circumvent the possible complication of the ROP2 effect on RIC1 localization (Fu et al., 2005), we analyzed YFP-RIC1

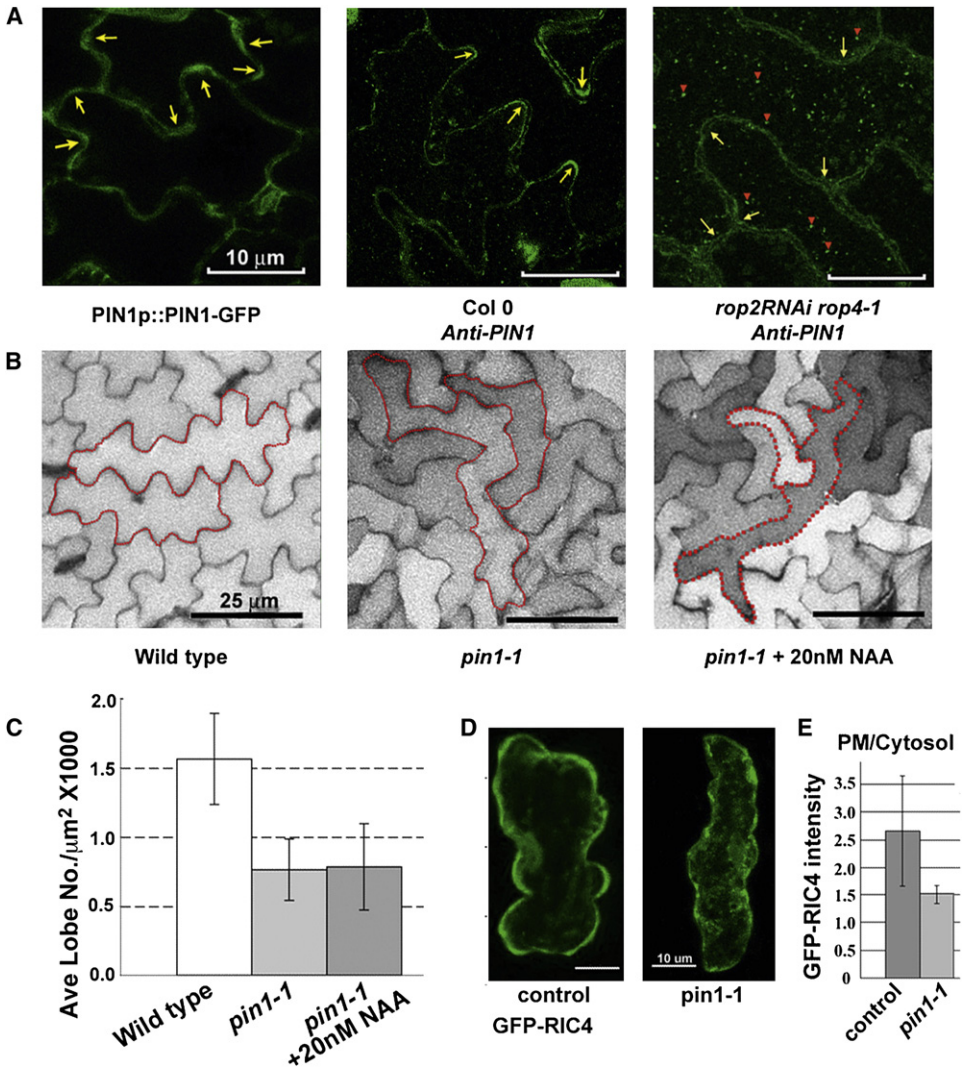

Figure 5. PIN1 Is Localized to the Lobe Tip and Is Essential for Auxin Promotion of PC Interdigitation

(A) Left: PIN1-GFP was preferentially localized to the tip of lobes in PC. Middle: Immunostaining of PIN1 in PCs. Arrows indicates the accumulation of PIN1 at the lobe region. Right: Immunostaining of PIN1 in *ROP2RNAi rop4-1* mutant. Arrows (yellow) indicates the accumulation of PIN1 at the lobe region was lost in *ROP2RNAi rop4-1*. Arrowheads indicate internalized PIN1, which was greatly increased in the cytoplasm of *ROP2RNAi rop4-1* cells. 75 cells from 3 repeats are used for quantification (Figure S5H).

(B) PC shapes in wild-type (left) and *pin1-1* mutant (middle). *pin1-1* PCs were slender with few lobes, a phenotype similar to a *rop2-1rop4-1* double knockout mutant (data not shown). 20 nM NAA was unable to rescue *pin1-1* phenotype in PCs (right).

(C) Quantitative data for (B). Lobe numbers per cell area in *pin1-1* mutant and *pin1-1* mutant treated with 20 nM NAA were quantified using double blind analysis as described in Figure. S3. *pin1-1* cells showed significantly reduced lobe formation compared to wide type ($n = 400$, t test $p < 0.001$), and 20 nM NAA did not rescue this phenotype ($n = 400$, t test $p > 0.1$). Higher NAA concentrations had no effect on the *pin1-1* phenotype either (Figures S5A and S5B).

(D) GFP-RIC4 distribution pattern in PCs of wild-type and *pin1-1* mutant. GFP-RIC4 was localized to the cell cortex preferentially in lobe tips or lobe emergent sites of wild-type PCs but was mostly diffuse in the cytosol in *pin1-1* PCs.

(E) Quantitative analysis of the cortical GFP-RIC4 signal was performed as described in Figure. S2. Cortical signal of GFP-RIC4 dramatically decreased in *pin1-1* mutant ($n > 25$, t test $p < 0.001$).

Also see Figure S5.

localization in the *rop2-1 rop4-1* mutant, in which ROP2 function is compromised. YFP-RIC1 appeared as beads lining cortical MTs (Figures 6C and 6D) (Fu et al., 2005). Ten minutes after the application of 10 nM NAA, the number of YFP-RIC1 associated MTs increased, and MTs became more ordered, especially in the indented region of the PC (Figure 6D). Furthermore, both the number of YFP-RIC1 beads and their intensity greatly increased as rapidly as 4 min after NAA application (Figures 6E and 6F). In *abp1-5*, auxin failed to change the localization pattern of RIC1 (Figures 6D–6G), suggesting that ABP1 acts upstream of ROP6. These results support the hypothesis that auxin activates the ROP6-RIC1 pathway in an ABP1-dependent manner.

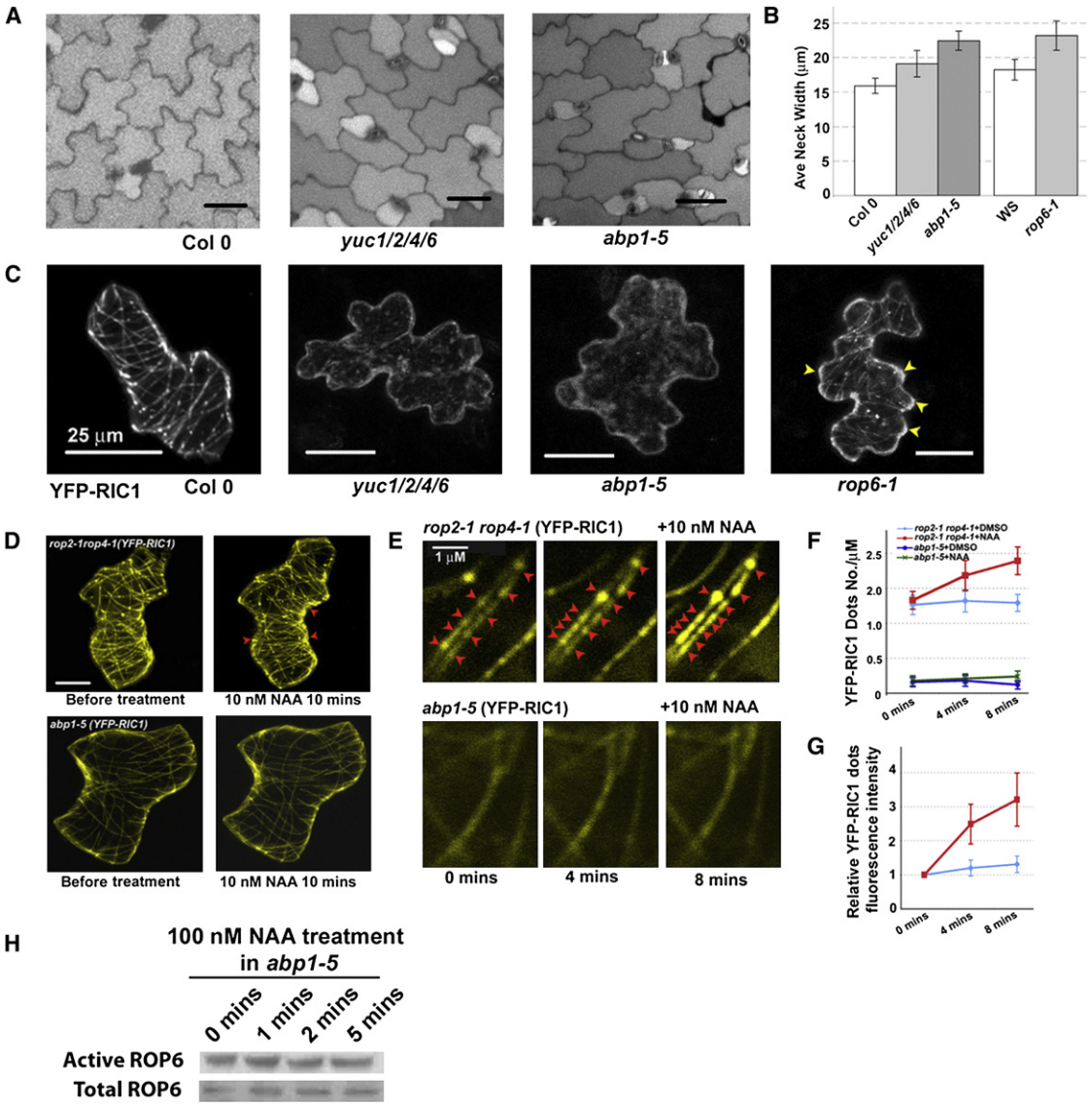

Figure 6. Auxin Activates the ROP6-RIC1 Pathway through ABP1

(A) PCs in both *yuc1/2/4/6* and *abp1-5* have wider neck regions than WT, similar to both *rop6-1* and *ric1-1* mutants (Fu et al., 2009, 2005), but different from *ROP2RNAi rop4-1,* which has a narrower neck (Fu et al., 2005).

(B) Quantitative analysis of PCs phenotype showed that both *yuc1/2/4/6* (t test, $p < 0.01$) and *abp1-5* (t test, $p < 0.001$) had significantly wider neck regions than WT. Data are mean neck width ± SD ($n > 400$ cells).

(C) YFP-RIC1 formed dot-like structures along cortical MTs in WT cells (left) (Fu et al., 2005, 2009). In *yuc1/2/4/6* and *abp1-5* cells, YFP-RIC1 lost its association with MTs as in *rop6-1* ($n > 25$). In *rop6-1* mutants, YFP-RIC1 was mostly shifted to lobe regions (indicated by arrowheads) where ROP2 was presumably activated. This YFP-RIC1 localization pattern is different from that in the *yuc1/2/4/6* and *abp1-5* mutants, where YFP-RIC1 became diffusely localized to the cytosol because ROP2 is inactivated in these mutants.

(D) Auxin enhanced YFP-RIC1 association with cortical MTs in a *rop2-1 rop4-1* mutant, but not in the *abp1-5* mutant. PCs transiently YFP-RIC1 were treated with NAA (10 nM) and imaged by confocal microscopy before and 10 min after treatment. In *rop2-1 rop4-1* PCs, YFP-RIC1 was associated with MTs in a beads-on-a-string pattern. NAA enhanced this localization pattern as indicated by arrowheads. In *abp1-5* cells, the weak YFP-RIC1 association with MTs did not show the dotted pattern and was not altered by NAA treatment. At least 15 cells were tracked for each mutant and showed similar response to NAA. The scale bar represents 10 μm.

(E) A time-course analysis of YFP-RIC1 association with MTs. At 4 and 8 min after NAA treatment, YFP-RIC1 dots gradually increased in both intensity and number by auxin treatment in *rop2-1 rop4-1* but not *abp1-5* cells.

(F and G). Quantitative analysis of YFP-RIC1 dot number and intensity shown in (D) and (E). (F) YFP-RIC1 association with MTs was measured by the number of YFP-RIC1 dots unit length of MTs. Data are mean dot number per μm ± SD ($n = 50$). (G) Average intensity of YFP-RIC1 dots was measured from 0 min to 8 min. The intensity at time 0 was standardized as 1. Data are relative mean intensity compared to time 0 ± SD ($n = 100$).

(H). Auxin failed to increase ROP6 activity in *abp1-5* muants. GTP-bound GFP-ROP6 in protoplasts isolated from a *abp1-5* line stably expressing *35S::GFP-ROP6* was analyzed as described in Figure 2.

Also see Figure S6.

Auxin Activates ROP6 Rapidly

To further confirm auxin activation of the ROP6-RIC1 pathway, we determined the effect of auxin on ROP6 activity. Indeed, auxin treatments increased the amount of active ROP6 in a dosage-dependent manner (Figures 2A and 2B). The range of NAA concentrations for ROP6 activation was similar to that for ROP2 activation, but the saturation of ROP6 activation required higher NAA levels. Like ROP2, ROP6 was rapidly activated within 30 s after 100 nM NAA treatment (Figures 2C and 2D), consistent with a role for ABP1 in the perception of auxin that activates ROP6. ABP1-dependent ROP6 activation by auxin was further demonstrated by our finding that the auxin-dependent increase in ROP6 activity was abolished by the *abp1-5* mutation (Figure 6H). The activation of two antagonizing ROPs (ROP2 and ROP6) by the same auxin perception system with a similar auxin response range but distinct saturation kinetics may provide a mechanism for the localized activation of ROP2 and ROP6 in the complementary lobing and indenting sides by uniformly applied auxin (see Discussion).

DISCUSSION

The findings here have several important implications. First, these results establish a cytoplasmic auxin-signaling mechanism that is distinct from the TIR1-based nuclear auxin-signaling pathway and provides a perspective of auxin action at the cellular level. Second, our findings give insights into hormonal signaling leading to changes in the cytoskeleton and vesicular trafficking, which is crucial for hormone action in plants yet scarcely studied. Third, we show that ABP1 acts upstream of ROP GTPase signaling, which gives an unprecedented understanding of signaling events downstream of the auxin perception by ABP1, whose mode of action has been long sought for. Finally, our results suggest that the ABP1- and ROP-dependent auxin signaling plays a pivotal role in the spatial coordination of cell expansion within and between cells during interdigitated growth of PCs. Since auxin is a multifunctional hormone polarly transported out of cells, this auxin-signaling mechanism could serve as a common mode of intracellular and intercellular coordination of cell growth, morphogenesis and polarity in plants.

An Auxin-Signaling Mechanism Regulates Cytoplasmic Pathways

The TIR1/AFB-dependent nuclear auxin-signaling system is essential for auxin-mediated growth, development, and patterning that rely changes in gene expression (Dharmasiri et al., 2005a, 2005b; Kepinski and Leyser, 2005; Mockaitis and Estelle, 2008). Previous work hints toward the existence of other auxin-signaling mechanisms (Badescu and Napier, 2006), and our findings here clearly establish a distinct auxin-signaling mechanism that exists in the cell boundary/cytoplasm and is capable of responding to auxin in seconds. Complementary to the TIR1 nuclear pathway impacting auxin-mediated gene expression, the ABP1/ROP-dependent pathways directly regulate cytoplamsic events such as actin and microtubule organization and PIN protein trafficking. Thus, our findings shed light into the dark box of the mechanism by which auxin modulates cytoskeletal reorganization and cell morphogenesis in multicellular tissues of plants. Although our work here focuses on the roles of this auxin-signaling mechanism in PC interdigitation, it is likely that similar ABP1-ROP signaling pathways may operate in other plant cells and tissues because of widespread expression and functions of ABP1 and ROPs in plants (Braun et al., 2008; Chen et al., 2001a, 2001b; Fu et al., 2005, 2002, 2009; Jones, 1994; Jones and Herman, 1993; Jones et al., 1998).

Our findings here do not exclude the involvement of ROPs in the regulation of TIR1/AFB-dependent auxin responses. In fact, it was shown in tobacco and *Arabidopsis* protoplasts that expression of dominant-negative or constitutively active forms of the tobacco NtRac1 ROP affected auxin-induced gene expression (Tao et al., 2002), and thus ROP may also regulate the nuclear pathway in addition to the cytoplasmic pathways.

ABP1 May Be a Cell-Surface Auxin Receptor that Activates ROP2 and ROP6 Signaling

Here, we show ABP1 is required for the rapid activation of PM-localized ROP2 and ROP6 by auxin. ABP1 is partially associated with the outer surface of the PM through its binding to a GPI-anchored protein (Shimomura, 2006), and the cell surface-associated ABP1 mediates auxin activation of cell expansion (Chen et al., 2001a; Jones et al., 1998). Hence we propose that ABP1 may be a cell surface receptor of auxin that controls PC interdigitation. This is also consistent with our finding that PIN1-mediated auxin export is required for ROP2 activation. ABP1 is not a transmembrane protein and likely works with a transmembrane partner or coreceptor, whose identification will be crucial for understanding how auxin is perceived at the cell surface and how it leads to ROP activation in the cytoplamic side of the PM.

A Working Model for the Coordination of Interdigitated Cell Growth and Beyond

We propose a working model for the auxin signaling pathways required for interdigitated growth (i.e., development of complementary lobes and indentations) in PCs (Figure 7). In this paper, we demonstrate that ABP1-mediated auxin perception activates both of the ROP2 and ROP6 pathways, which were previously shown to be locally activated at opposing sides of the cell wall but mutually exclusive along the PM within a PC (Fu et al., 2005, 2009; Yang, 2008). At the steady state, therefore, simultaneous activation of ROP2 and ROP6 by localized extracellular auxin must occur at the opposing sites (lobe and indentation bordered by the cell wall) but not at the same site. A key aspect of this working model is the existence of an auxin-ROP2-PIN1-auxin positive feedback loop, which acts together with the antagonizing ROP6 pathway to generate the presumed localized extracellular auxin. Importantly, this working model can explain how extracellular auxin coordinates lobe and indentation development at the steady state, once the interdigitation pattern has been initiated (i.e., the cell region for lobe formation or indentation has already been established).

Positive feedback loop initiated by a stochastic local change in Rho GTPase signaling has been proposed to be a mechanism for the establishment of self-organizing cell polarity in yeast and animal cells (Altschuler et al., 2008; Hazak et al., 2010; Paciorek et al., 2005; Van Keymeulen et al., 2006; Xu et al.,

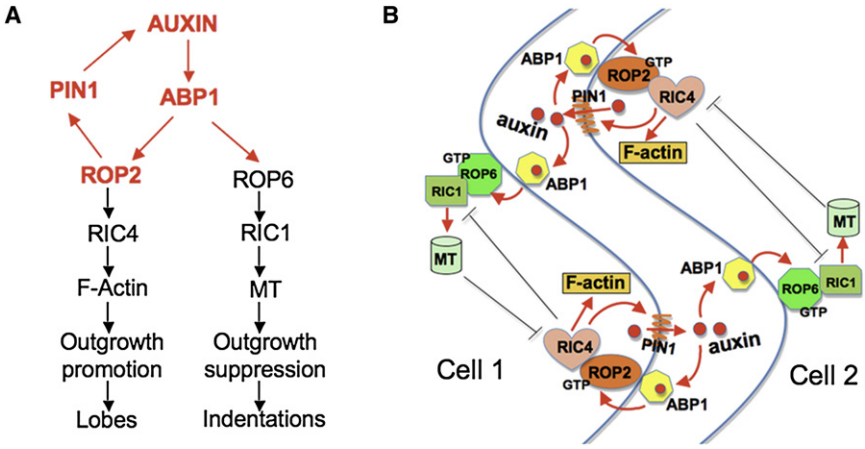

Figure 7. A Working Model for Auxin Control of Interdigitated Cell Growth

(A) A model for coordination of two ROP signaling pathways by localized extracellular auxin, which results from a PIN1-mediated positive feedback loop.

(B) A model for auxin control of interdigitated growth through inter- and intra-cellular coordination of the ROP2 and ROP6 pathways. We surmise that the PC intergditated growth is controlled by an auxin-dependent self-organizing mechanism. In this mechanism, localized extracellular auxin, which is generated by self-activation via the auxin→ROP2→PIN1→auxin feedback loop and self-maintenance via the antagonizing ROP6 pathway, controls cell-cell coordination of lobing and indentating by activating the complementary ROP2 and ROP6 pathways in two adjacent cells, which are mutually exclusive within each cell to allow for the formation of alternating lobes and indentations (Fu et al., 2005, 2009).

2003). In neutrophil and other animal cells, the perception of uniform concentrations of chemoattractants by a single receptor leads to establishment of the frontness and backness polarity by activating two antagonistic cytoskeleton-regulating Rho GTPase pathways (Hazak et al., 2010; Paciorek et al., 2005; Van Keymeulen et al., 2006; Xu et al., 2003). Similarly, the activation of the antagonistic ROP2 and ROP6 pathways by the ABP1 perception of uniform concentrations of auxin could also explain how uniformly applied auxin leads to the establishment of cell cortical regions that define lobe- or indentation-forming sites to initiate the interdigitation pattern (Figures 1 and 7). Therefore the self-organization design principles for the spatial coordination of cell growth and movement might be conserved in both single and multicellular tissue across eukaryotic kingdoms.

Our working model may serve as a unifying mechanism for the coordination of cell morphogenesis and polarity within various plant tissues. Auxin appears to orchestrate PIN polarization in files of cells directing auxin flow (Paciorek et al., 2005; Sauer et al., 2006) and in coordinating hair positioning in root-hair-forming cells (Fischer et al., 2006). The position of root hair formation can be predicted by the polar localization of ROP2 in the hair forming cells (Jones et al., 2002), and ROP2 polar localization is affected by auxin (Fischer et al., 2006; Yang, 2008), raising the possibility that the auxin-mediated ROP signaling may also underlie the coordination of polar cell growth among root epidermal cells.

Our working model here could also be used to explain how auxin may coordinate the polarization of PIN proteins to the same cell end among a file of cells that direct auxin flow, i.e., auxin could activate a ROP2-like pathway that forms a positive feedback loop at the end of PIN localization as well as a ROP6-like pathway that antagonizes with the ROP2-like pathway at the side lacking PIN localization. Auxin was shown to inhibit PIN internalization in root cells (Dhonukshe et al., 2008; Paciorek et al., 2005), which is also in agreement with our finding in this report that PIN1 internalization is increased when ROP2 function is compromised in PCs. In further support of a role for ROP signaling in the modulation of PIN polarization, Interactor of Constitutively active ROP 1 (ICR1), a likely ROP effector protein, was recently found to regulate PIN polarization both in *Arabidopsis* embryonic and root cells (Hazak et al., 2010). Importantly, ABP1 is shown to affect PIN protein localization in root cells and other types (Robert et al., 2010 [this issue of *Cell*]), providing strong argument for a general role of the ABP1-ROP signaling in the modulation of PIN polarization. Therefore we anticipate that the elucidation of the ROP-based cytoplasmic auxin signaling pathways in various auxin-mediated processes will likely be an exciting and fertile area of research in cell and developmental biology in the coming years.

EXPERIMENTAL PROCEDURES

Plant Materials and Growth Conditions

Arabidopsis plants were grown at 22°C on MS agar plates or in soil with 16 hr light/8 hr dark cycles unless indicated otherwise. The *DR5::GUS* line and the *yuc1 yuc2 yuc4 yuc6* quadruple mutant were kindly provided by Tom Guilfoyle and Yunde Zhao, respectively (Cheng et al., 2006; Hagen and Guilfoyle, 2002). The double-mutant *ROP2RNAi rop4-1* line was described previously (Fu et al., 2005). The *pin1-1* and *pin1-5* mutants are T-DNA insertional lines obtained from ABRC (SALK, CS8065, and 097144, respectively) and their genotypes were confirmed by PCR analysis.

The *abp1-5* allele contains a missense mutation of C→G in the 94 codon of the coding sequence. Tilling mutant *abp1-5* was backcrossed 6 times with Col-0 and genotyped by restriction digestion of PCR fragments (see Supplemental Information for details). For genetic complementation, *abp1-5* was transformed with the *Arabidopsis* wild-type ABP1 cDNA driven by the 35S promoter.

Conditional plants for ABP1 expression were obtained by expressing either a full-length antisense construct or the recombinant single-chain fragment variable 12 derived from the monoclonal anti-ABP1 antibody mAb12 under the control of the ethanol inducible system as described (Braun et al., 2008; David et al., 2007). Ethanol induction was obtained by exposure of siblings to ethanol vapor generated from 500 μl of 5% ethanol in a microtube placed at the bottom of sealed square plate.

Confocal and Imprinting Analysis of Leaf *Arabidopsis* PC Shape

PC shape from *Arabidopsis* cotyledons was imaged directly on confocal microscopy (Leica SP2) or indirectly by an imprinting method (Mathur and

Koncz, 1997). Since PCs are auto-fluorescent, their cell outlines can be imaged on confocal microscopy with the following settings: excitation 351 nm or 364 nm, 50% laser power and emission 400-600 nm. For some treatments, the cotyledons were curved, so analyzing cell shapes by confocal microscopy was difficult. In this case, an agarose imprinting method was used (Mathur and Koncz, 1997), and .cell outlines imprinted on the agarose were imaged on bright field microscopy (Nikon). Additional image analyses involved use of Metamorph 4.5. The images are edited by photoshop 7.0 by adjusting figure sizes and resolution and adding labels.

Ballistics-Mediated Transient Expression in Leaf Epidermal Cells

Subcellular localization of GFP-RIC4, YFP-RIC1 and F-actin was analyzed by use of transiently-expressed *pBI221:GFP-RIC4, pUC:YFP-RIC1* and *pBI221:GFP-mTalin* constructs as described previously (Fu et al., 2005, 2002). We used 0.8 μg *pBI221:GFP-mTalin*, 1 μg *pBI221:GFP-RIC4* and 1 μg *pUC:YFP-RIC1* for particle bombardment. GFP and YFP signal was detected 5 hr after bombardment by use of a Leica SP2 microscope (GFP: 488 nm excitation, 25% power; excitation 520–600 nm, gain at 600; YFP: 514 nm excitation, 25% power; excitation 530–600 nm, gain at 600). Cells at stage II showing similar medium levels of GFP (Fu et al., 2005, 2002) were chosen for GFP marker analysis. For 3D reconstruction, optical sections in 1.0 μm increments were imaged for each cell by use of the Leica software.

Naphthalene-1-Acetic Acid Treatments

Naphthalene-1-acetic acid (NAA) (Sigma, St. Louis, MO) was dissolved in DMSO as 0.5 M stock solutions, which were diluted to the indicated concentrations in liquid MS (for seedling treatments) or W5 media (for protoplast treatments). Seeds were germinated in the liquid MS media containing NAA or NPA. Each treatment was repeated at least three times with the corresponding controls.

Protoplast Preparation and PEG-Mediated Transient Expression

Protoplast preparation and PEG-mediated transient expression were described previously (Sheen, 2001). The 2nd or 3rd pair of rosette leaves from 2- or 3-week-old seedlings was used to prepare protoplasts. Protoplasts were counted by use of a hemacytometer (Hausser scientific, Cat # 1483). An amount of 10^5–10^6 protoplasts were used for ROP2 activity assay, and10^4–10^5 protoplasts were used for transient expression.

ROP2 and ROP6 Activity Assays in Protoplasts

Two different methods were used to analyze auxin activation of ROP2 in protoplasts. The first method involves a biochemical assay, in which GFP-tagged active ROP2 or ROP6 was pulled down by use of MBP-RIC1. Protoplasts were isolated from leaves of 2- or 3-week old *35S::GFP-ROP2* or –ROP6 transgenic seedlings as described previously (Jones et al., 2002; Sheen, 2001). Isolated protoplasts were treated with different concentrations of NAA, or with 100 nM for various times and frozen by liquid nitrogen. Total protein was extracted from 10^5–10^6 treated protoplasts. Twenty micrograms of MBP-RIC1-conjugated agarose beads were added to the protoplast extracts, and incubated at 4°C for 3 hr. The beads were washed three times at 4°C (5 min each). GTP-bound GFP-ROP2 or -ROP6 that was associated with the MBP-RIC1 beads was used for analysis by western blotting with an anti-GFP antibody (Santa Cruz Biotechnology, Santa Cruz, CA). Prior to the pull-down assay, a fraction of total proteins was analyzed by immunoblot assay to determine total GFP-ROP2 or -ROP6 (GDP-bound and GTP-bound). The amount of GTP-bound ROPs was normalized to that of total ROPs. The level of GTP-bound ROPs relative to the control (0 nM NAA at 0 min) was calculated by dividing the amount of normalized GTP-bound ROP2 or ROP6 from each treatment by the normalized amount from the control, which is defined as "1."

In the second method, changes in GFP-RIC4 localization to the PM were monitored in isolated protoplasts. Protoplasts were isolated from leaves of wild-type plants (Col 0) or mutants as described above. Two micrograms of a *35S::GFP-RIC4* construct was introduced into 10^4-10^5 protoplasts by PEG-mediated transformation. Typically, 70%–80% of the protoplasts were transformed. Protoplasts were incubated at 23°C for 5 hr to overnight, treated with NAA (1 μM final concentration), and imaged immediately by use of a Leica SP2 confocal microscope. The earliest possible time for imaging was 2 min after NAA application. Time-lapse images were taken every 2–3 min.

Quantitative Analysis of GFP-RIC4 and YFP-RIC1 Localization

The images of GFP-RIC4 localization in both PCs and protoplasts were taken by Leica SP2, and image analysis were conducted by Metamorph 4.5 using region function. First we created a region along cell cortex. The average intensity of GFP for this was calculated by Metamorph. Then we created a region just inside of the cell cortex, which included all cytoplasm signals, and the average cytoplasmic signal was calculated. The average signals were then used to calculate the ratio of PM/Cyto.

YFP-RIC1 was transiently expressed in PCs using the ballistics-mediated method as described above. Four to five hours after bombardments, leaves were treated with 10 nM NAA, and time-series YFP-RIC1 images are taken using a Leica SP2 confocal microscope 2 min after treatement. The average intensity of YFP-RIC1 dots along MT and the length of MT bundle were directly measured by the Metamorph software, and the number of YFP-RIC1 dots was counted by eyeballing. YFP-RIC1 dots No./μm indicates the number of YFP-RIC1 dots divided by MT length.

Immunolocalization of PIN1, RIC1, and MT in PCs

Whole-mount immunostaining of *Arabidopsis* leaves was previously described (Fu et al., 2005; Wasteneys et al., 1997). Fixed, shattered and permeabilized leaves were incubated with primary antibody (anti-PIN1 1:200, anti-RIC1 1:100, anti-αTubulin 1:200) overnight at 4°C (Paciorek et al., 2005), and then incubated with the second antibody (FITC conjugated anti-rabbit IgG 1:200, TRITC conjugated anti-mouse IgG 1:200) for 2 hr at 37°C. Stained cells were observed in Leica SP2 confocal microscope. Cells at stage II (Fu et al., 2005, 2002) were chosen for comparison between wild-type and mutant cells.

SUPPLEMENTAL INFORMATION

Supplemental Information includes Extended Experimental Procedures and six figures and can be found with this article online at doi:10.1016/j.cell.2010.09.003.

ACKNOWLEDGMENTS

We are grateful to Veronica Grieneisen, Ben Scheres, Athanasius F. M. Marée, Paulien Hogeweg, Xuemei Chen, and G. Venugopala Reddy for their stimulating discussion and critical comments on this manuscript; and to Xinping Cui for her assistance with the statistical analysis. We are grateful to Tom Guilfoyle and Yunde Zhao for their generous supply of *Arabidopsis* mutant lines used in this work. This work is supported by grants from the U.S. National Institute of General Medical Sciences to Z.Y. (GM081451) and to A.M.J. (GM065989), by the National Science Foundation to A.M.J. (MCB-0718202) and the Department of Energy to A.M.J. (DE-FG02-05ER15671) and to Z.Y. (DE-FG02-04ER15555) and by the Research Foundation-Flanders (Odysseus) to J.F.

Received: March 13, 2010
Revised: June 2, 2010
Accepted: July 30, 2010
Published: September 30, 2010

REFERENCES

Abel, S., and Theologis, A. (1996). Early genes and auxin action. Plant Physiol. *111*, 9–17.

Altschuler, S.J., Angenent, S.B., Wang, Y., and Wu, L.F. (2008). On the spontaneous emergence of cell polarity. Nature *454*, 886–889.

Badescu, G.O., and Napier, R.M. (2006). Receptors for auxin: will it all end in TIRs? Trends Plant Sci. *11*, 217–223.

Baxter-Burrell, A., Yang, Z., Springer, P.S., and Bailey-Serres, J. (2002). RopGAP4-dependent Rop GTPase rheostat control of Arabidopsis oxygen deprivation tolerance. Science *296*, 2026–2028.

Braun, N., Wyzykowaska, J., Couch, D., David, K., Muller, P., Perrot-Rechenmann, C., and Fleming, A.J. (2008). Conditional Repression of AUXIN BINDING PROTEIN 1 Shows That It Is Required During Post-Embryonic Shoot Development and Implicates ABP1 as a Co-ordinator of Cell Division and Cell Expansion. Plant Cell *20*, 2746–2762.

Chen, J.G., Shimomura, S., Sitbon, F., Sandberg, G., and Jones, A.M. (2001a). The role of auxin-binding protein 1 in the expansion of tobacco leaf cells. Plant J. *28*, 607–617.

Chen, J.G., Ullah, H., Young, J.C., Sussman, M.R., and Jones, A.M. (2001b). ABP1 is required for organized cell elongation and division in Arabidopsis embryogenesis. Genes Dev. *15*, 902–911.

Cheng, Y., Dai, X., and Zhao, Y. (2006). Auxin biosynthesis by the YUCCA flavin monooxygenases controls the formation of floral organs and vascular tissues in Arabidopsis. Genes Dev. *20*, 1790–1799.

David, K.M., Couch, D., Braun, N., Brown, S., Grosclaude, J., and Perrot-Rechenmann, C. (2007). The auxin-binding protein 1 is essential for the control of cell cycle. Plant J. *50*, 197–206.

Dharmasiri, N., Dharmasiri, S., and Estelle, M. (2005a). The F-box protein TIR1 is an auxin receptor. Nature *435*, 441–445.

Dharmasiri, N., Dharmasiri, S., Weijers, D., Lechner, E., Yamada, M., Hobbie, L., Ehrismann, J.S., Jurgens, G., and Estelle, M. (2005b). Plant development is regulated by a family of auxin receptor F box proteins. Dev. Cell *9*, 109–119.

Dhonukshe, P., Tanaka, H., Goh, T., Ebine, K., Mahonen, A.P., Prasad, K., Blilou, I., Geldner, N., Xu, J., Uemura, T., et al. (2008). Generation of cell polarity in plants links endocytosis, auxin distribution and cell fate decisions. Nature *456*, 962–966.

Diekmann, W., Venis, M.A., and Robinson, D.G. (1995). Auxins induce clustering of the auxin-binding protein at the surface of maize coleoptile protoplasts. Proc. Natl. Acad. Sci. USA *92*, 3425–3429.

Fischer, U., Ikeda, Y., Ljung, K., Serralbo, O., Singh, M., Heidstra, R., Palme, K., Scheres, B., and Grebe, M. (2006). Vectorial information for Arabidopsis planar polarity is mediated by combined AUX1, EIN2, and GNOM activity. Curr. Biol. *16*, 2143–2149.

Fu, Y., Gu, Y., Zheng, Z., Wasteneys, G., and Yang, Z. (2005). Arabidopsis interdigitating cell growth requires two antagonistic pathways with opposing action on cell morphogenesis. Cell *120*, 687–700.

Fu, Y., Li, H., and Yang, Z. (2002). The ROP2 GTPase controls the formation of cortical fine F-actin and the early phase of directional cell expansion during Arabidopsis organogenesis. Plant Cell *14*, 777–794.

Fu, Y., Xu, T., Zhu, L., Wen, M., and Yang, Z. (2009). A ROP GTPase signaling pathway controls cortical microtubule ordering and cell expansion in Arabidopsis. Curr. Biol. *19*, 1827–1832.

Green, J.B., and Davidson, L.A. (2007). Convergent extension and the hexahedral cell. Nat. Cell Biol. *9*, 1010–1015.

Hagen, G., and Guilfoyle, T. (2002). Auxin-responsive gene expression: genes, promoters and regulatory factors. Plant Mol. Biol. *49*, 373–385.

Hazak, O., Bloch, D., Poraty, L., Sternberg, H., Zhang, J., Friml, J., and Yalovsky, S. (2010). A rho scaffold integrates the secretory system with feedback mechanisms in regulation of auxin distribution. PLoS Biol. *8*, e1000282.

Heasman, J. (2006). Patterning the early Xenopus embryo. Development *133*, 1205–1217.

Hwang, J.U., Gu, Y., Lee, Y.J., and Yang, Z. (2005). Oscillatory ROP GTPase activation leads the oscillatory polarized growth of pollen tubes. Mol. Biol. Cell *16*, 5385–5399.

Jones, A.M. (1994). Auxin-binding proteins. Annu. Rev. Plant Physiol. Plant Mol. Biol. *45*, 393.

Jones, A.M., and Herman, E. (1993). KDEL-containing, auxin-binding protein is secreted to the plasma membrane and cell wall. Plant Physiol. *101*, 595–606.

Jones, A.M., Im, K.H., Savka, M.A., Wu, M.J., DeWitt, N.G., Shillito, R., and Binns, A.N. (1998). Auxin-dependent cell expansion mediated by overexpressed auxin-binding protein 1. Science *282*, 1114–1117.

Jones, M.A., Shen, J.J., Fu, Y., Li, H., Yang, Z., and Grierson, C.S. (2002). The Arabidopsis Rop2 GTPase is a positive regulator of both root hair initiation and tip growth. Plant Cell *14*, 763–776.

Kepinski, S., and Leyser, O. (2005). The Arabidopsis F-box protein TIR1 is an auxin receptor. Nature *435*, 446–451.

Leblanc, N., David, K., Grosclaude, J., Pradier, J.M., Barbier-Brygoo, H., Labiau, S., and Perrot-Rechenmann, C. (1999). A novel immunological approach establishes that the auxin-binding protein, Nt-abp1, is an element involved in auxin signaling at the plasma membrane. J. Biol. Chem. *274*, 28314–28320.

Leyser, O. (2006). Dynamic integration of auxin transport and signalling. Curr. Biol. *16*, R424–R433.

Mathur, J., and Koncz, C. (1997). Method for preparation of epidermal imprints using agarose. Biotechniques *22*, 280–282.

Mockaitis, K., and Estelle, M. (2008). Auxin receptors and plant development: A new signaling paradigm. Annu. Rev. Cell Dev. Biol. *24*, 55–80.

Paciorek, T., Zazimalova, E., Ruthardt, N., Petrasek, J., Stierhof, Y.D., Kleine-Vehn, J., Morris, D.A., Emans, N., Jurgens, G., Geldner, N., et al. (2005). Auxin inhibits endocytosis and promotes its own efflux from cells. Nature *435*, 1251–1256.

Parry, G., and Estelle, M. (2006). Auxin receptors: a new role for F-box proteins. Curr. Opin. Cell Biol. *18*, 152–156.

Petrasek, J., Mravec, J., Bouchard, R., Blakeslee, J.J., Abas, M., Seifertova, D., Wisniewska, J., Tadele, Z., Kubes, M., Covanova, M., et al. (2006). PIN proteins perform a rate-limiting function in cellular auxin efflux. Science *312*, 914–918.

Robert, S., Kleine-Vehn, J., Barbez, E., Sauer, M., Paciorek, T., Baster, P., Vanneste, S., Zhang, J., Simon, S., Covanová, M., et al. (2010). ABP1 mediates auxin inhibition of clathrin-dependent endocytosis in *Arabidopsis*. Cell *143*, this issue, 111–121.

Sauer, M., Balla, J., Luschnig, C., Wisniewska, J., Reinohl, V., Friml, J., and Benkova, E. (2006). Canalization of auxin flow by Aux/IAA-ARF-dependent feedback regulation of PIN polarity. Genes Dev. *20*, 2902–2911.

Senn, A.P., and Goldsmith, M.H. (1988). Regulation of Electrogenic Proton Pumping by Auxin and Fusicoccin as Related to the Growth of Avena Coleoptiles. Plant Physiol. *88*, 131–138.

Settleman, J. (2005). Intercalating Arabidopsis leaf cells: a jigsaw puzzle of lobes, necks, ROPs, and RICs. Cell *120*, 570–572.

Sheen, J. (2001). Signal transduction in maize and Arabidopsis mesophyll protoplasts. Plant Physiol. *127*, 1466–1475.

Shimomura, S. (2006). Identification of a Glycosylphosphatidylinositol-anchored Plasma Membrane Protein Interacting with the C-terminus of Auxin-binding Protein 1: A Photoaffinity Crosslinking Study. Plant Mol. Biol. *60*, 663–677.

Shishova, M., and Lindberg, S. (2004). Auxin induces an increase of Ca2+ concentration in the cytosol of wheat leaf protoplasts. J. Plant Physiol. *161*, 937–945.

Steffens, B., Feckler, C., Palme, K., Christian, M., Bottger, M., and Luthen, H. (2001). The auxin signal for protoplast swelling is perceived by extracellular ABP1. Plant J. *27*, 591–599.

Tan, X., Calderon-Villalobos, L.I., Sharon, M., Zheng, C., Robinson, C.V., Estelle, M., and Zheng, N. (2007). Mechanism of auxin perception by the TIR1 ubiquitin ligase. Nature *446*, 640–645.

Tao, L.Z., Cheung, A.Y., and Wu, H.M. (2002). Plant Rac-like GTPases are activated by auxin and mediate auxin-responsive gene expression. Plant Cell *14*, 2745–2760.

Van Keymeulen, A., Wong, K., Knight, Z., Govaerts, C., Hahn, K., Shokat, K., and Bourne, H. (2006). To stabilize neutrophil polarity, PIP3 and Cdc42 augment RhoA activity at the back as well as signals at the front. J. Cell Biol. *174*, 437–445.

Vanneste, S., and Friml, J. (2009). Auxin: a trigger for change in plant development. Cell *136*, 1005–1016.

Wasteneys, G.O., Willingale-Theune, J., and Menzel, D. (1997). Freeze shattering: a simple and effective method for permeabilizing higher plant cell walls. J. Microsc. *188*, 51–61.

Wisniewska, J., Xu, J., Seifertova, D., Brewer, P.B., Ruzicka, K., Blilou, I., Rouquie, D., Benkova, E., Scheres, B., and Friml, J. (2006). Polar PIN localization directs auxin flow in plants. Science *312*, 883.

Woo, E.J., Marshall, J., Bauly, J., Chen, J.G., Venis, M., Napier, R.M., and Pickersgill, R.W. (2002). Crystal structure of auxin-binding protein 1 in complex with auxin. EMBO J. *21*, 2877–2885.

Xu, J., Wang, F., Van Keymeulen, A., Herzmark, P., Straight, A., Kelly, K., Takuwa, Y., Sugimoto, N., Mitchison, T., and Bourne, H. (2003). Divergent Signals and Cytoskeletal Assemblies Regulate Self-Organizing Polarity in Neutrophils. Cell *114*, 201–214.

Yang, Z. (2008). Cell polarity signaling in Arabidopsis. Annu. Rev. Cell Dev. Biol. *24*, 551–575.

Zhao, Y., Christensen, S.K., Fankhauser, C., Cashman, J.R., Cohen, J.D., Weigel, D., and Chory, J. (2001). A role for flavin monooxygenase-like enzymes in auxin biosynthesis. Science *291*, 306–309.